A Modified Proportional Navigation Guidance for Range Estimation

A. Moharampour*, J. Poshtan* and A. Khaki-Sedigh**

Abstract: In this paper, after defining pure proportional navigation guidance in the 3-dimensional state from a new point of view, range estimation for passive homing missiles is explained. Modeling has been performed by using line of sight coordinates with a particular definition. To obtain convergent estimates of those state variables involved particularly in range channel and unavailable from IR trackers, nonlinear filters such as sequential U-D extended Kalman filter and Unscented Kalman filter in modified spherical coordinate combined with a modified proportional navigation guidance law are proposed. Simulation results indicate that the proposed tracking filters in conjunction with the dual guidance law are able to provide the convergence of the range estimate for both maneuvering and non-maneuvering targets.

Keywords: IR Homing Missile, Pure Proportional Navigation Guidance, Range Estimation, Unscented Kalman Filter.

1 Introduction

Estimation of the relative distance between a missile and a target is among the most important quantities required for air defense missiles. This estimate maybe used either to compute the lead bias in developing of the traditional proportional navigation guidance (PNG) for gyro-stabilized IR trackers ([1, 2]) or to switch the tracking algorithms for imagining IR trackers.

In [3] an optimal recursive Bayesian filters applied directly to the nonlinear target model and particle filter approach is compared to a range parametized extended Kalman filter. In [4] a range estimation algorithm for Anti-Aircraft Artillery which operated by man is proposed and probability matrix computed for state transition after modeling filter state under the measurement failure probability.

The PNG has been widely recognized as an efficient guidance scheme for homing missiles. In this scheme, the acceleration command given to the missile is proportional to the angular rate of the line of sight (LOS) between the missile and the target. The PNG law has been shown to be optimal in the sense that it minimizes the integral of the square of the missile acceleration needed to intercept the target. Based on the direction of the commanded acceleration, the PNG is usually classified into two types: pure proportional navigation guidance (PPNG), and true proportional navigation guidance (TPNG). In [5], PPNG and TPNG are compared from the viewpoints of implementation and pursuit behavior. In TPNG, the commanded acceleration is directed perpendicular to LOS. In PPNG, however the commanded acceleration is directed perpendicular to the velocity vector of the missile. In [6], it has been shown via a Lyapanov-like method in a 3-dimensional case that a missile guided by the PPNG law can always intercept a target maneuvering with random time-varying vertical acceleration, provided that: 1) the target acceleration varies within a known band; 2) the navigation constant is chosen sufficiently large; 3) the missile is launched with a small initial heading error or the missile is kept forward to the target during the flight.

In [7] an extended Kalman filter (EKF) in modified spherical coordinate (MSC) in a 2-dimensional case, combined with a modified proportional navigation guidance (MPNG) law is utilized to obtain convergent estimates of state variables involved in range channel and unavailable from IR trackers. In [8], it has been proposed a guidance law to enhance observability in 3-dimensional engagements.

In this paper, after defining PPNG in 3-dimensional state from a new point of view, range estimation for passive homing missiles is explained. Modeling has been performed by using LOS coordinates with a particular definition. Using this LOS coordinates the

Iranian Journal of Electrical & Electronic Engineering, 2008.
Paper first received 27th November 2007 and in revised form 17th May 2007.
* The Authors are with the Department of Electrical Engineering, Iran University of Science & Technology, 16844, Narmak, Tehran, Iran.
E-mail: mo_afr@iust.ac.ir, jposhtan@iust.ac.ir.
** The Author is with the Department of Electrical Engineering, K. N. Toosi University of Technology, Seyyed Khandan Bridge, Shariati Street, P.O. Box: 16315-1355, Tehran, Iran.
E-mail: sedigh@kntu.ac.ir.

acceleration command is simply explained in missile coordinates, making it most appropriate for single-channel missiles. The state-space relations in a 3-dimensional case is explained by using target-missile dynamics. To obtain convergent estimates of those state variables involved particularly in range channel and unavailable from IR trackers, nonlinear filters such as sequential U-D EKF and Unscented Kalman filter (UKF) in MSC combined with a MPNG law are proposed. Measurements used include the LOS and the reverse of time-to-go, those that the missile is practically capable of measuring. The proposed guidance law is the traditional PPNG in which an additional term comprising a cross range compensator [9], is used to provide and improve the observability of trajectory and obtain convergent estimates of state variables. Simulation results indicate that the proposed tracking filters in conjunction with the dual guidance law are able to provide the convergence of the range estimate for both maneuvering and non-maneuvering targets.

2 Dynamics Equations

Suppose that $\vec{r}_m$ and $\vec{r}_t$ are respectively location vectors of the missile and the target in inertial coordinate system $\{I\}$. Hence the LOS vector is defined as

$$\vec{r} = \vec{r}_t - \vec{r}_m \tag{1}$$

By taking derivative of the above equation, we will have

$$\dot{\vec{r}} = \vec{v}_t - \vec{v}_m \tag{2}$$

$$\ddot{\vec{r}} = \vec{a}_t - \vec{a}_m \tag{3}$$

If $\vec{\Omega}$ is assumed to be the rotation vector of $\vec{r}$ with respect to inertial coordinates, then

$$\vec{\Omega} = \frac{\vec{r} \times (\vec{v}_t - \vec{v}_m)}{r^2} \tag{4}$$

in which $r = \|\vec{r}\|$ is the Euclidean norm of $\vec{r}$.

Definition 1: The LOS coordinate system $\{L\}$ is defined such that its x_L axis lies along $\vec{r}$, z_L lies along $\vec{\Omega}$, and y_L axis is chosen so that the resulting is right-handed coordinate system [10]. The $x_L y_L$ plane is called as the instantaneous engagement plane (see Fig. 1). If we indicate unit vectors along x_L, y_L and z_L with $\vec{l}_r$, $\vec{l}_t$ and $\vec{l}_\Omega$ respectively, then we will have

$$\vec{l}_\Omega = \vec{\Omega}/\omega \;,\; \omega = \|\vec{\Omega}\| \quad , \quad \vec{l}_t = \vec{l}_\Omega \times \vec{l}_r \tag{5}$$

Also, Eq. (2) can be rewritten as

$$\vec{V}_g = \begin{cases} -N\vec{v}_c(0) \text{ or } N\vec{v}_{ri} & \text{for TPNG} \\ -N\vec{v}_m & \text{for PPNG} \end{cases} \tag{6}$$

Now from Eq. (2) and Eq. (6) we will obtain

$$\dot{r} = v_{tx} - v_{mx} \tag{7}$$

$$r\omega = v_{ty} - v_{my} \tag{8}$$

$$0 = v_{tz} - v_{mz} \tag{9}$$

where (v_{tx}, v_{ty}, v_{tz}) are components of the target velocity vector, and (v_{mx}, v_{my}, v_{mz}) are components of the missile velocity vector defined in the $\{L\}$ coordinate system. Also the derivative of Eq. (6) yields

$$\ddot{\vec{r}} = (\ddot{r} - r\omega^2)\vec{l}_r + (r\dot{\omega} + 2\omega\dot{r})\vec{l}_t + r\omega\omega_{\|}\vec{l}_\Omega \tag{10}$$

where $\omega_{\|}$ is the component of $\vec{\omega}_{IL}$ along the x-axis in $\{L\}$. Consequently from Eq. (3) and Eq. (10), we will obtain

$$\ddot{r} - r\omega^2 = a_{tx} - a_{mx} \tag{11}$$

$$r\dot{\omega} + 2\omega\dot{r} = a_{ty} - a_{my} \tag{12}$$

$$r\omega\omega_{\|} = a_{tz} - a_{mz} \tag{13}$$

where (a_{tx}, a_{ty}, a_{tz}) are components of the target acceleration vector and (a_{mx}, a_{my}, a_{mz}) are components of the missile acceleration vector defined in $\{L\}$ coordinate system.

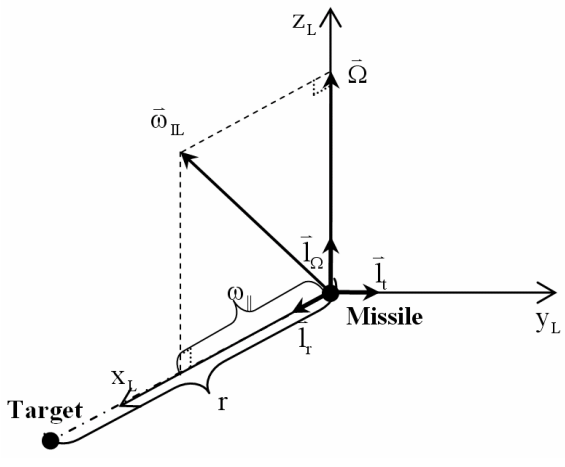

Fig. 1 LOS coordinate system.

Theorem 1: suppose that $\vec{\Omega}$ is the rotation vector of $\vec{r}$ relative to the inertial coordinate system. Then by defining the LOS coordinate system $\{L\}$, the following results will be obtained:

a. The second vector component of $\vec{\omega}_{IL}^{L}$ (LOS angular rate vector defined in the $\{L\}$ coordinate system) is zero.

b. The engagement plane is rotating with a velocity equal to the value of the first component of $\vec{\omega}_{IL}^{L}$, and this value is proportional to the subtraction of the third components of the target and the missile accelerations.

c. The value of the third components of the target and the missile velocity vectors in the $\{L\}$ coordinate system will be equal.

d. The missile commanded acceleration from TPNG or PPNG, has no component perpendicular to the instantaneous engagement plane.

Proof: Assume that $\vec{\omega}_{IL}^{L}$ has three components as follows:

$$\vec{\omega}_{IL}^{L} = \omega_{\|}\,\vec{l}_r + \omega_t\,\vec{l}_t + \omega\vec{l}_\Omega \tag{14}$$

Noting that

$$\begin{aligned}\dot{\vec{l}}_r &= \vec{\omega}_{IL} \times \vec{l}_r \\ &= -\omega_t\,\vec{l}_\Omega + \omega\vec{l}_r\end{aligned} \tag{15}$$

By taking into account the Eq. (6) and Eq. (15) we obtain

$$\begin{aligned}\dot{\vec{r}} &= \dot{r}\,\vec{l}_r + r\,\dot{\vec{l}}_r \\ &= \dot{r}\,\vec{l}_r + r\omega\vec{l}_t - r\omega_t\,\vec{l}_\Omega\end{aligned} \tag{16}$$

On the other hand, from Eq. (6) we obtain

$$\begin{aligned}\vec{r}\times\dot{\vec{r}} &= \vec{r}\times(\vec{\omega}\times\vec{r}) \\ &= r^2\omega\vec{l}_\Omega\end{aligned} \tag{17}$$

Besides, according to Eq. (16) we obtain

$$\vec{r}\times\dot{\vec{r}} = r^2\omega_t\,\vec{l}_t + r^2\omega\vec{l}_\Omega \tag{18}$$

By comparing the Eq. (17) and Eq. (18), we will get

$$\omega_t = 0 \tag{19}$$

and hence part **a** of the theorem is proved. Part **b** is obtained from Eq. (13). In fact, the engagement plane is rotating at $\omega_{\|}$ velocity. In other words, if third components of the target and the missile accelerations are equal, then the engagement plane will hold constant. Part **c** is obvious from Eq. (9). We prove part **d** for both TPNG and PPNG. In the 3-dimentional case, the missile commanded acceleration is explained as follows [11]

$$\vec{a}_{mc} = \vec{V}_g \times \vec{\Omega} \tag{20}$$

where we have

$$\vec{V}_g = \begin{cases} -N\,\vec{v}_c(0) \;\text{ or }\; N\,\vec{v}_{ri} & \text{for TPNG} \\ -N\,\vec{v}_m & \text{for PPNG}\end{cases} \tag{21}$$

In Eq. (21) N is the navigation constant, and $\vec{v}_{ri}$ is a predetermined constant vector in the engagement plane and is independent from initial conditions [12]. Then Eq. (21) can be simplified as

$$\vec{V}_g = \begin{cases} (N\dot{r})\,\vec{l}_r & \text{for TPNG} \\ -N\left[(v_{mx})\,\vec{l}_r + (v_{my})\,\vec{l}_t + (v_{mz})\,\vec{l}_\Omega\right] & \text{for PPNG}\end{cases} \tag{22}$$

In the case when the missile uses the TPNG method, considering the definition of $\vec{\Omega}$ in Eq. (4), and from Eq. (6), Eq. (20) and Eq. (22), the missile commanded acceleration can be defined in $\{L\}$ coordinate system as

$$\vec{a}_{mc}^{L} = -(N\dot{r}\omega)\,\vec{l}_t \tag{23}$$

In the case when the missile uses the PPNG method, from Eq. (20) and Eq. (22) the missile commanded acceleration is defined in $\{L\}$ coordinate system as

$$\vec{a}_{mc}^{L} = -(N\omega\,v_{my})\,\vec{l}_r + (N\omega\,v_{mx})\,\vec{l}_t \tag{24}$$

Now from Eq. (23) and Eq. (24) it is clear that in both TPNG and PPNG cases, the missile has no control component perpendicular to the instantaneous engagement plane. Hence part **d** is also proved.

Now we define the missile coordinate system $\{M\}$ and the target coordinate system $\{T\}$ using Euler angles [6]. For the sake of simplicity, we assume that the missile and the target are mass points, and that the missile seeker and autopilot have dynamics fast enough to be ignored. The target-missile engagement geometry in the 3-dimentional case has been shown in Fig. 2. The missile angular rate vector relative to the LOS defined

in the missile coordinate system has the following form [6]

$$\vec{\omega}_{LM}^{M} = \dot{\psi}_m \; S\theta_m \vec{i}_M - \dot{\theta}_m \vec{j}_M + \dot{\psi}_m \; C\theta_m \vec{k}_M \qquad (25)$$

where $S\theta_m = \sin(\theta_m)$ and $C\theta_m = \cos(\theta_m)$. On the other hand, we know that

$$\vec{a}_m = \vec{\omega}_{IL} \times \vec{v}_m + \vec{\omega}_{LM} \times \vec{v}_m \qquad (26)$$

Therefore

$$\vec{a}_m^M = (C_L^M \vec{\omega}_{IL}^L) \times \vec{v}_m^M + \underline{\omega}_{LM}^M \times \vec{v}_m^M \qquad (27)$$

where C_L^M is transformation Matrix from $\{L\}$ to $\{M\}$. Also, by ignoring the attack angle, assume that both the target and the missile velocity vectors have components only along the x-axis of their own coordinate systems. That is

$$\begin{aligned} \vec{v}_m^M &= v_m \vec{i}_M \\ \vec{v}_t^T &= v_t \vec{i}_T \end{aligned} \qquad (28)$$

($\vec{i}_M, \vec{j}_M$ and $\vec{k}_M$ are unit vectors along x_M, y_M and z_M respectively and also $\vec{i}_T, \vec{j}_T$ and $\vec{k}_T$ are unit vectors along x_T, y_T and z_T respectively). Using Eq. (14), Eq. (25) and Eq. (28), we can rewrite Eq. (27) as follows

$$\begin{aligned} \vec{a}_m^M = &\left[v_m(\dot{\psi}_m + \omega) C\theta_m - \omega_{\|} S\theta_m C\psi_m \right] \vec{j}_M \\ &+ v_m(\dot{\theta}_m + \omega_{\|} S\psi_m) \vec{k}_M \end{aligned} \qquad (29)$$

On the other hand, by expressing the PPNG law, referred to in Eq. (20) and Eq. (21), in the missile coordinate, we obtain

$$\vec{a}_m^M = C_L^M \vec{a}_{mc}^L = N v_m \omega C\theta_m \vec{j}_M \qquad (30)$$

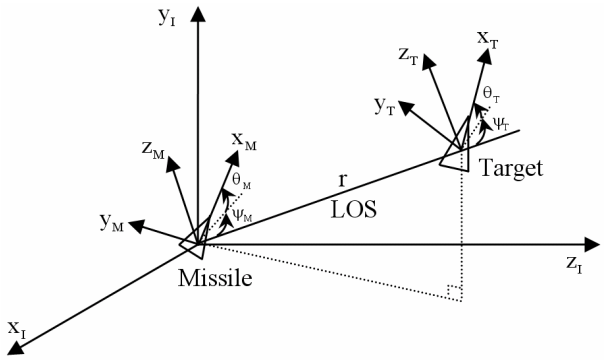

Fig. 2 The target-missile engagement geometry.

That is to say, in the 3-dimentional PPNG, and with respect to the expressed $\{M\}$ and $\{L\}$ coordinate systems, it is simply sufficient for the missile to have acceleration command component only in the direction of y-axis of the missile body coordinate system. ω is measured by the seeker and θ_m can be calculated out of seeker gimbal's angles. This kind of explanation is much simpler than expressing the missile acceleration vector in the LOS coordinate system defined only by Euler angles [6]. If we denote this acceleration by a_{my}^M, then we will have from Eq. (30)

$$a_{my}^M = N v_m \omega C\theta_m \qquad (31)$$

The following equations will also be obtained from the equality of the right hand sides of Eq. (29) and Eq. (30)

$$\begin{aligned} \dot{\theta}_m &= -\omega_{\|} S\psi_m \\ \dot{\psi}_m &= \frac{a_{my}^M}{v_m C\theta_m} - \omega + \frac{\omega_{\|} \tan\theta_m C\psi_m}{v_m} \end{aligned} \qquad (32)$$

Besides, by using Eq. (13) and regarding the fact that the third component of missile acceleration in the LOS coordinate system is zero according to Eq. (30), we obtain the following

$$\omega_{\|} = \frac{a_{tz}}{r\omega} \qquad (33)$$

3 Modified Proportional Navigation Guidance

Passive homing guidance laws for IR missiles are commonly based on PNG or APNG if the target acceleration is available. However, it is shown in [9] that neither PNG nor APNG provide observability to target tracking systems with LOS only measurements. [9] Suggests a modified augmented PNG law which includes a cross range deviation term to provide initial LOS angle oscillation without sacrificing terminal guidance effectiveness. In this study, we propose the same cross range term for the modification of guidance law.

Theorem 2: If the missile acceleration command is modified as expressed in Eq. (34), then the initial oscillation of the LOS angle is provided without affecting the terminal guidance phase.

$$\vec{a}_m^M = (N v_m \omega C\theta_m + \frac{Fr\sigma}{C\psi_m}) \vec{j}_M \qquad (34)$$

where F is a positive constant, and σ is the LOS angle such that $\dot{\sigma} = \omega$ and it is measured in the Cartesian coordinates with the x-axis along the initial LOS to the target so that $\sigma(0) = 0$.

Proof: The missile acceleration command, given in Eq. (30), may be expressed as follows in the LOS coordinate system

$$\begin{aligned}\vec{a}_m^{L} = &\left[-Nv_m\omega C\theta_m S\psi_m - Fr\sigma\tan(\psi_m)\right]\vec{i}_M \\ &+\left[Nv_m\omega\, C\theta_m C\psi_m + Fr\sigma\right]\vec{j}_M\end{aligned} \tag{35}$$

Considering the missile-target relative dynamics according to Eq. (12), we will get

$$r\ddot{\sigma} - 2v_c\dot{\sigma} = a_{ty} - N'v_c\dot{\sigma}C\theta_m C\psi_m - Fr\sigma \tag{36}$$

where $v_c = -\dot{r}$ is the closing velocity and $N' = Nv_m/v_c$. Besides, we know that

$$t_{go} = -\frac{r}{\dot{r}} \tag{37}$$

Hence, assuming the time-to-go, defined as $t_{go} \triangleq t_f - t$, where t_f is the flight terminal phase time, we obtain from Eq. (36)

$$\ddot{\sigma} + \frac{(N'C\theta_m C\psi_m - 2)}{(t_f - t)}\dot{\sigma} + F\sigma = \frac{a_{ty}}{v_c(t_f - t)} \tag{38}$$

For large values of t_{go}, Eq. (38) can be rewritten as

$$\ddot{\sigma} + F\sigma = 0 \tag{39}$$

which indicates that a dominant $F\sigma$ term provides oscillatory motion of σ. when $t_{go} \to 0$, the second term in the left side of Eq. (37) is dominant and hence the terminal performance will be similar to the PPNG law. F is selected to provide natural frequency of the LOS angle oscillation and the oscillation can be induced by the initial missile heading error inherent to passive homing missile even for a non-maneuvering target. Hence theorem 2 is proved. During simulation, F= 0.1 is selected, which results in an oscillatory motion of σ with natural frequency of 0.05 Hz. Therefore, the proposed guidance law takes the following form

$$\vec{a}_m^{M} = \left[Nv_m\omega\, C\theta_m + \frac{Fr\sigma}{C\psi_m}\right]\vec{j}_M \tag{40}$$

Since parameters θ_m, ψ_m, r and σ may not be measured by the system, for practical implementation, these variables are replaced by estimated values from a state estimator. Hence the MPNG law can be proposed as follows

$$\vec{a}_m^{M} = \left[Nv_m\omega\, C\hat{\theta}_m + \frac{F\hat{r}\hat{\sigma}}{C\hat{\psi}_m}\right]\vec{j}_M \tag{41}$$

4 Practical Computation of t_{go}

IR seekers possess IR intensity measuring units at their detector outlet. The IR intensity of an IR point source is of the following form [13]

$$V_{out} = \frac{D^*_{max}V_n}{(A_d\Delta f)^{\frac{1}{2}}}\cdot\frac{LA_1A_2}{r^2}k \tag{42}$$

where V_{out} is the output signal voltage, V_n is the noise signal voltage, D^*_{max} is the detectivity, A_d is the electric bandwidth of the equivalent noise, Δf is equivalent noise bandwidth, L is the transmittance constant, A_1 is the radiating body area, A_2 is the detector area, r is the source range to the detector, and k is the radiation intensity constant of the source. With respect to the availability of the AGC circuit, this voltage can be put into the following form

$$V_{out} = \overline{K}/r^2 \tag{43}$$

where $\overline{K}$ is a constant parameter. By differentiating Eq. (43), we obtain

$$\dot{V}_{out} = -\frac{\overline{2K}\dot{r}}{r^3} \tag{44}$$

Now, t_{go} is simply obtained from Eq. (43) and Eq. (44) by

$$t_{go} = \frac{2}{\left(\frac{\dot{V}_{out}}{V_{out}}\right)} \tag{45}$$

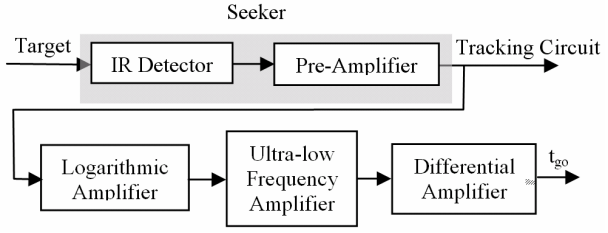

Fig. 3 Practical implementation for t_{go} calculation.

In practical implementation to compute this value, a logarithmic amplifier and then a differentiator are arranged after the detector output (See Fig. 3).

5 State Estimation

The choice of coordinate system is crucial for nonlinear filters because the coupling between different coordinates (or states) can seriously degrade their performance. In this paper, a sequential U-D EKF estimator [14] in the MSC has been utilized to estimate the required variables for the implementation of MPNG algorithm expressed in Eq. (41). A major virtue of the MSC approach is that it decouples the relatively accurate states from the downrange states, which prevents covariance matrix ill-conditioning. Thus, the inaccurate range will not appear in the equations to update the covariance matrices, which is an important advantage of MSC [15].

The state vector in MSC is defined as

$$\begin{aligned}\bar{x} &= (\sigma, \omega, \theta_m, \psi_m, \frac{1}{r}, \frac{\dot{r}}{r}, a_{tx}^L, a_{ty}^L, a_{tz}^L) \\ &= (x_1, x_2, x_3, x_4, x_5, x_6, x_7, x_8, x_9)\end{aligned} \tag{46}$$

The continuous system dynamics are represented as follows

$$\dot{\bar{x}} = \bar{f}\left(\bar{x}, \bar{w}, \bar{a}_m^M\right) \tag{47}$$

Using Eq. (11), Eq. (12), Eq. (13), Eq. (32) and Eq. (33), the state space equations in scalar form can be put in the following form

$$\begin{aligned}
\dot{x}_1 &= x_2 \\
\dot{x}_2 &= -2x_2x_6 + x_5(x_8 - a_{my}^M \cos x_4) \\
\dot{x}_3 &= -\frac{x_5x_9}{x_2}\sin x_3 \\
\dot{x}_4 &= -x_2 + \frac{x_5x_9}{x_2}\frac{\tan x_3 \cos x_4}{v_m} + \frac{a_{my}^M}{v_m \cos x_3} \\
\dot{x}_5 &= -x_5x_6 \\
\dot{x}_6 &= x_2^2 - x_6^2 + x_5(x_7 + a_{my}^M \sin x_4) \\
\dot{x}_7 &= w_1 \\
\dot{x}_8 &= w_2 \\
\dot{x}_9 &= w_3
\end{aligned} \tag{48}$$

where a_{my}^M is the component of the missile acceleration along the y-axis in $\{M\}$ coordinate system, and (w_1, w_2, w_3) are Gaussian process noises with the following characteristics

$$\begin{aligned}
&\bar{w} = (w_1, w_2, w_3) \\
&E(w_1) = 0, E(w_2) = 0, E(w_3) = 0 \\
&E\left(\bar{w}(\zeta_2), \bar{w}(\zeta_1)\right) = \sigma_T^2 \delta(\zeta_2 - \zeta_1) I_{3\times 3}
\end{aligned} \tag{49}$$

where σ_T^2 is the variance of the process noise. Accordingly, the state equations for state estimation in MSC are as follows

$$\dot{\hat{\bar{x}}} = \bar{f}\left(\hat{\bar{x}}, \bar{0}, \bar{a}_m^M\right) \tag{50}$$

The linear differential equation for the state estimation error is given by

$$\begin{aligned}
\dot{\tilde{\bar{x}}} &= \dot{\bar{x}} - \dot{\hat{\bar{x}}} \\
&= F\tilde{\bar{x}} + G\bar{w}
\end{aligned} \tag{51}$$

where the linearized plant matrix is given by

$$F = \left.\frac{\partial \bar{f}}{\partial \bar{x}}\right|_{\bar{x}=\hat{\bar{x}}} = \begin{bmatrix}
0 & 1 & 0 & 0 & 0 & 0 & 0 & 0 & 0 \\
0 & -2x_6 & 0 & F_{2,4} & F_{2,5} & -2x_2 & 0 & x_5 & 0 \\
0 & F_{3,2} & 0 & F_{3,4} & F_{3,5} & 0 & 0 & 0 & F_{3,9} \\
0 & F_{4,2} & F_{4,3} & F_{4,4} & F_{4,5} & 0 & 0 & 0 & F_{4,9} \\
0 & 0 & 0 & 0 & -x_6 & -x_5 & 0 & 0 & 0 \\
0 & 2x_2 & 0 & F_{6,4} & F_{6,5} & -2x_6 & x_5 & 0 & 0 \\
0 & 0 & 0 & 0 & 0 & 0 & 0 & 0 & 0 \\
0 & 0 & 0 & 0 & 0 & 0 & 0 & 0 & 0 \\
0 & 0 & 0 & 0 & 0 & 0 & 0 & 0 & 0
\end{bmatrix} \tag{52}$$

where

$$\begin{aligned}
&F_{2,4} = x_5 a_{my}^M \sin x_4, F_{2,5} = x_8 - a_{my}^M \cos x_4 \\
&F_{3,2} = \frac{x_5x_9}{x_2^2}\sin x_4, F_{3,4} = -\frac{x_5x_9}{x_2}\cos x_4, F_{3,5} = -\frac{x_9}{x_2}\sin x_4 \\
&F_{3,9} = -\frac{x_5}{x_2}\sin x_4, F_{4,2} = -1 - \frac{x_5x_9}{v_m x_2^2}\tan x_3 \cos x_4 \\
&F_{4,3} = \frac{a_{my}^M}{v_m \cos^2 x_3}\sin x_3 + \frac{x_5x_9}{v_m x_2}(1 + \tan^2 x_3)\cos x_4 \\
&F_{4,4} = -\frac{x_5x_9}{v_m x_2}\tan x_3 \sin x_4, F_{4,5} = \frac{x_9}{v_m x_2}\tan x_3 \cos x_4 \\
&F_{4,9} = \frac{x_5}{v_m x_2}\tan x_3 \cos x_4, F_{6,4} = x_5 a_{my}^M \cos x_4 \\
&F_{6,5} = x_7 + a_{my}^M \sin x_4
\end{aligned} \tag{53}$$

The process noise input matrix G_w is defined as

$$G_w = \left.\frac{\partial \bar{f}}{\partial \bar{w}}\right|_{\bar{x}=\hat{\bar{x}}} = \begin{bmatrix} 0 & 0 & 0 & 0 & 0 & 0 & 1 & 0 & 0 \\ 0 & 0 & 0 & 0 & 0 & 0 & 0 & 1 & 0 \\ 0 & 0 & 0 & 0 & 0 & 0 & 0 & 0 & 1 \end{bmatrix}^T \quad (54)$$

Then the time update of the state error covariance is computed as

$$M_{i|i-1} = \Phi(t_i, t_{i-1}) P_{i-1|i-1} \Phi^T(t_i, t_{i-1}) + Q_i \quad (55)$$

where $P_{i|i}$ is the updated measurement of the error covariance after the i-th measurement, Φ is the state transition matrix, and Q_i is the process noise covariance matrix, defined as

$$\Phi(T_s, 0) = I + FT_s \quad (56)$$

$$Q_i = E\int_{t_{i-1}}^{t_i}\int_{t_{i-1}}^{t_i} \Phi(t_i,\zeta_2) G_w(\zeta_2) \bar{w}(\zeta_2) \bar{w}^T(\zeta_1) G_w{}^T(\zeta_1) \Phi^T(t_i,\zeta_1) d\zeta_1 d\zeta_2$$

$$= aT_s \begin{bmatrix} 0 & 0 & 0 & 0 & 0 & 0 & 0 & 0 & 0 \\ 0 & Q_{2,2} & 0 & 0 & 0 & 0 & 0 & Q_{2,8} & 0 \\ 0 & 0 & Q_{3,3} & Q_{3,4} & 0 & 0 & 0 & 0 & Q_{3,9} \\ 0 & 0 & Q_{4,3} & Q_{4,4} & 0 & 0 & 0 & 0 & Q_{4,9} \\ 0 & 0 & 0 & 0 & 0 & 0 & 0 & 0 & 0 \\ 0 & 0 & 0 & 0 & 0 & Q_{6,6} & Q_{6,7} & 0 & 0 \\ 0 & 0 & 0 & 0 & 0 & Q_{7,6} & 1 & 0 & 0 \\ 0 & Q_{8,2} & 0 & 0 & 0 & 0 & 0 & 1 & 0 \\ 0 & 0 & Q_{9,3} & Q_{9,4} & 0 & 0 & 0 & 0 & 1 \end{bmatrix} \quad (57)$$

where

$$Q_{2,2} = \frac{1}{3}T_s^2 \hat{x}_5^2 \quad , \quad Q_{2,8} = \frac{1}{2}T_s \hat{x}_5$$

$$Q_{3,3} = \frac{1}{3}\left(T_s \frac{\hat{x}_5}{\hat{x}_2}\right)^2 \sin^2 \hat{x}_4$$

$$Q_{3,4} = -\frac{1}{3}\left(T_s \frac{\hat{x}_5}{\hat{x}_2}\right)^2 \sin \hat{x}_4 \tan \hat{x}_3 \cos \hat{x}_4$$

$$Q_{3,9} = -\frac{1}{2}T_s \frac{\hat{x}_5}{\hat{x}_2} \sin \hat{x}_4 \quad , \quad Q_{4,3} = Q_{3,4} \quad (58)$$

$$Q_{4,4} = \frac{1}{3}\left(T_s \frac{\hat{x}_5}{\hat{x}_2}\right)^2 \tan^2 \hat{x}_3 \cos^2 \hat{x}_4$$

$$Q_{4,9} = \frac{1}{2}T_s \frac{\hat{x}_5}{\hat{x}_2} \tan \hat{x}_3 \cos \hat{x}_4$$

$$Q_{6,6} = Q_{2,2} \quad , \quad Q_{6,7} = Q_{7,6} = Q_{8,2} = Q_{2,8}$$

$$Q_{9,3} = Q_{3,9} \quad , \quad Q_{9,4} = Q_{4,9}$$

and [16]

$$a = n_T^2 / t_f \quad (59)$$

where n_T is the target maneuverability, t_f is the time of flight for the homing phase. T_s is the sampling time for the process discretization. We also have

$$P_{i|i} = (I - K_i H_i) M_{i|i-1} (I - K_i H_i)^T + K_i R_i K_i^T \quad (60)$$

where K_i the Kalman gain matrix is defined as

$$K_i = M_{i|i-1} H_i^T (H_i M_{i|i-1} H_i^T + R_i)^{-1} \quad (61)$$

In the above, the measurement matrix H_i and the measurement noise covariance R_i can be defined from the following measurement equation

$$Z_i = H_i \bar{x}_i + \bar{v}_i \quad (62)$$

$$H = \begin{bmatrix} 0 & 1 & 0 & 0 & 0 & 0 & 0 & 0 & 0 \\ 0 & 0 & 0 & 0 & 0 & 1 & 0 & 0 & 0 \end{bmatrix} \quad (63)$$

Here, it has been assumed that the first measurement is the LOS rotation rate measured by the seeker, and the second measurement is accessible with respect to Eq. (45) and t_{go} measurement procedure depicted in Fig. 3. Besides, the measurement noise $\bar{v}_i$ is assumed to be additive, white and Gaussian with the following characteristics

$$E(\bar{v}_i) = \bar{0} \quad , \quad R_i = E(\bar{v}_i \bar{v}_i{}^T) = \begin{bmatrix} \sigma_\omega^2 & 0 \\ 0 & \sigma_{\frac{\dot{r}}{r}}^2 \end{bmatrix} \quad (64)$$

where $(\sigma_\omega^2, \sigma_{\frac{\dot{r}}{r}}^2)$ are the standard deviations for the LOS rate and $\dot{r}/r$ parameter, and [17]

$$\sigma_{\frac{\dot{r}}{r}}^2 = \left(\frac{1}{r}\right)^2 \sigma_{\dot{r}}^2 + \left(\frac{1}{r}\right)^2 \left(\frac{\dot{r}}{r}\right)^2 \sigma_r^2 \quad (65)$$

Finally, after the i-th measurement, the updating of the state estimate in MSC is given by

$$\hat{\bar{x}}_{i|i} = \hat{\bar{x}}_{i|i-1} + K_i (Z_i - H_i \hat{\bar{x}}_{i|i}) \quad (66)$$

In general, for practical realizations of the proposed filter, the sequential U-D extended Kalman technique is usually invoked to improve numerical accuracy and to maintain non-negativity and symmetry of the computed variance [14].

6 Unscented Kalman Filter (UKF)

This filter was first proposed in [18]. The UKF is an extended Kalman filter, which reduces the EKF linearization errors. EKF uses first-order linearization to update mean and covariance, but UKF uses unscented transformations instead of linearization to propagate mean and covariance and is more accurate. UKF approximates the posterior density $p(x_t \mid \mathbb{Y}_t)$ by a Gaussian density function, which is denoted by a set of given sample points. These sample points completely capture the mean and covariance of Gaussian density, and when propagated by nonlinear transformation, they cover mean and covariance up to the second order linearization. In fact, UKF performs a kind of statistical linearization instead of analytical linearization (as for EKF). In UKF there is no need to compute Hessian and Jacobian matrices which are used in EKF. It is similar to EKF from the view point of computational complexity. It is said that UKF is much more accurate than EKF, but in the articles where this advantage has been mentioned, EKF may not have been properly implemented [19].

For the implementation of this filter, at first the augmented state vector is formed as follows

$$x^a = [x_1, x_2, x_3, x_4, x_5, x_6, x_7, x_8, x_9, v_1, v_2, v_3, n_1, n_2]^T \quad (67)$$

where x_1 to x_9 are system state variables, v_1,v_2 and v_3 are process noises, and n_1 and n_2 are measurement noises. For the initialization of x^a, noise initial values are assumed to be zero. The covariance matrix of the initial error is defined as follows

$$P_0^a = \begin{bmatrix} P_0 & 0 & 0 \\ 0 & P_v & 0 \\ 0 & 0 & P_n \end{bmatrix} \quad (68)$$

where P_0 is as in EKF, and P_v and P_n are respectively the process and measurement covariance matrices.

In UKF, at first 2n+1 sigma points $\{\mathcal{X}^i\}_{i=0}^{2n}$ and their corresponding weights W^i are generated, and then are used with the unscented transform (UT) to perform the mean ($\hat{x}_k$) and covariance (P_k) calculations required in the Kalman framework. The UT weights are given in terms of the parameter $\lambda = \alpha^2(L+\kappa) - L$ and the prior knowledge parameter β. L is the vector length of x^a, α is used to control the spread of sigma points around the mean, and κ is the secondary scaling parameter. α, β, and κ are taken for simulation as 0.9 , 2 and 0 respectively. The sigma points are generated as follows [20]

$$\begin{aligned} &W_0^{(m)} = \lambda/L + \lambda, \quad W_0^{(c)} = W_0^{(m)} + \beta + 1 - \alpha^2 \\ &\mathcal{X}_{k-1}^a = \left[\hat{x}_{k-1|k-1}^a \quad \hat{x}_{k-1|k-1}^a \pm \left(\sqrt{(L+\lambda) P_{k-1|k-1}^a} \right)_i \right] \\ &W_i^{(m)} = W_i^{(c)} = 0.5/L + \lambda \quad i = 1, 2, \ldots, 2L \end{aligned} \quad (69)$$

where $\left(\left(\sqrt{.}\right)_i\right)$ is the i-th column of matrix square root. The time update equations are given by

$$\begin{aligned} &\mathcal{X}_{k|k-1}^x = f\left(\mathcal{X}_{k|k-1}^x, \mathcal{X}_{k|k-1}^v\right), \qquad \mathcal{Y}_{k|k-1} = h\left(\mathcal{X}_{k|k-1}^x, \mathcal{X}_{k|k-1}^n\right) \\ &\hat{x}_{k|k-1} = \sum_{i=0}^{2L} W_i^{(m)} \mathcal{X}_{i,k|k-1}^x, \qquad \hat{y}_{k|k-1} = \sum_{i=0}^{2n_y} W_i^{(m)} \mathcal{Y}_{i,k|k-1} \\ &P_{k|k-1} = \sum_{i=0}^{2L} W_i^{(c)} \left[\mathcal{X}_{i,k|k-1}^x - \hat{x}_{k|k-1}\right]\left[\mathcal{X}_{i,k|k-1}^x - \hat{x}_{k|k-1}\right]^T \end{aligned} \quad (70)$$

and the following relationship are used in the measurement update equations

$$\begin{aligned} &P_{xy} = \sum_{i=0}^{2L} W_i^{(c)} \left[\mathcal{X}_{i,k|k-1} - \hat{x}_{k|k-1}\right]\left[\mathcal{Y}_{i,k|k-1} - \hat{y}_{k|k-1}\right]^T \\ &P_{yy} = \sum_{i=0}^{2L} W_i^{(c)} \left[\mathcal{Y}_{i,k|k-1} - \hat{y}_{k|k-1}\right]\left[\mathcal{Y}_{i,k|k-1} - \hat{y}_{k|k-1}\right]^T \\ &\mathcal{K} = P_{xy} P_{yy}^{-1} \\ &\hat{x}_{k|k} = \hat{x}_{k|k-1} + \mathcal{K}\left(y_k - \hat{y}_{k|k-1}\right) \\ &P_{k|k} = P_{k|k-1} - \mathcal{K} P_{yy} \mathcal{K}^T \end{aligned} \quad (71)$$

where $x^a = [x^T \; v^T \; n^T]^T$ and $\mathcal{X}^a = [(\mathcal{X}^x)^T \; (\mathcal{X}^v)^T \; (\mathcal{X}^n)^T \;]^T$.

7 Simulation

In this section, the proposed MNPG law in Eq. (41) has been used in a Monte Carlo simulation for practical applications. The missile-target geometry depicted in Fig. 2 with various initial intercept conditions is utilized to set up engagement scenarios. The initial values for error covariance are adopted as follows [7]

$$\begin{aligned} &P_{0_{1,1}} = \sigma_\sigma^2, \sigma_\sigma = 0.026 \\ &P_{0_{2,2}} = \sigma_\omega^2, \sigma_\omega = 0.03 \\ &P_{0_{3,3}} = \sigma_{\theta_m}^2, \sigma_{\theta_m} = 0.087 \\ &P_{0_{4,4}} = \sigma_{\psi_m}^2, \sigma_{\psi_m} = 0.087 \\ &P_{0_{5,5}} = \sigma_r^2 \hat{x}_{0_5}^4, \sigma_r = 3000 \\ &P_{0_{6,6}} = \left[\sigma_{\dot{r}}^2 \hat{x}_{0_5}\right]^2 - 2C_{r\dot{r}}\sigma_r\sigma_{\dot{r}}\hat{x}_{0_5}^2\hat{x}_{0_6} \\ &\qquad + \left[\hat{x}_{0_5}\hat{x}_{0_6}\sigma_r\right]^2, \sigma_{\dot{r}} = 300, C_{r\dot{r}} = 0.5 \\ &P_{0_{5,6}} = -C_{r\dot{r}}\sigma_r\sigma_{\dot{r}}\hat{x}_{0_5}^3 + \hat{x}_{0_5}^3\hat{x}_{0_6}\sigma_r^2 \\ &P_{0_{6,5}} = P_{0_{5,6}} \\ &P_{0_{7,7}} = P_{0_{8,8}} = P_{0_{9,9}} = \sigma_T^2, \sigma_T = 40 \end{aligned} \quad (72)$$

The values of parameters are presented in Table 1. The simulation has been performed for three engagement scenarios: an accelerated target in head-on state, an accelerated target in tail-on state, and a non-accelerated target in tail-on state. These scenarios are as follows:

Table 1 Parameter values.

Parameter	Value	Description
T	0.01Sec	Sampling interval
V_m	450 m/s	Missile velocity
V_t	250 m/s	Target velocity
N	3.5	The effective navigation constant
F	0.1	The guidance constant in cross term
$\sigma(0)$	0 deg	The initial LOS angle
n_T	70 m/s^2	The target acceleration limit

1. **Launch scenario 1**: The first scenario represents an accelerated target on head-on aspect in which values of 3g have been considered for the target cross acceleration components but different initial estimate values have been considered for range, range rate, and the target acceleration components.
2. **Launch scenario 2**: The second scenario represents an accelerated target on tail-on aspect in which values of 3g have been considered for the components of target cross acceleration but different initial estimates have been considered for the range, range rate, and the target acceleration components.
3. **Launch scenario 3**: The third scenario represents a non-accelerated target on tail-on aspect. Again, different initial estimates for the range and the range rate have been considered.

The initial values of variables and the initial estimated values for each scenario are given in Table 2.

The performance of the proposed filters for each simulation run are calculated using root mean square error (RMSE) from the following [21]

$$\mathrm{RMSE}(t) = \sqrt{\frac{1}{N_{MC}} \sum_{j=1}^{N_{MC}} \left\| x_t^{True} - \hat{x}_t^{(j)} \right\|_2^2} \qquad (73)$$

where $N_{MC} = 50$ denotes the number of Monte Carlo simulations, and $\hat{x}_t^{(j)}$ denotes the estimation in instant *t* for j-th Monte Carlo simulation and x_t^{True} denotes the true value. The RMSE values are depicted in Figs. 4-6. The overall performance is calculated by the following equation

$$\mathrm{RMSE} = \sqrt{\frac{1}{L} \sum_{t=1}^{L} \sum_{j=1}^{N_{MC}} \left\| x_t^{True} - \hat{x}_t^{(j)} \right\|_2^2} \qquad (74)$$

Ignoring the transient state of range estimate, RMSE values for Monte Carlo simulations have been shown in Table 3. This values are obtained for $t \geq 2\,(\mathrm{Sec})$ have also been calculated. The UKF initializations are the same as EKF.

Table 2 Initial values for different scenarios.

	Scenario 1	Scenario 2	Scenario 3
$r(0)$	3000 m	1000 m	1000 m
$\hat{r}(0)$	10000 m	3000 m	3000 m
$\hat{\dot{r}}(0)$	-400 m/s	-200 m/s	-200 m/s
$\theta_t(0)$	10 deg	10 deg	10 deg
$\psi_t(0)$	135 deg	320 deg	320 deg
$\theta_m(0)$	20 deg	20 deg	20 deg
$\psi_m(0)$	20 deg	310 deg	310 deg
$a_{tx}(0)$	0	0	0
$a_{ty}(0)$	30 m/s^2	30 m/s^2	0
$a_{tz}(0)$	30 m/s^2	30 m/s^2	0
$\hat{a}_{tx}(0)$	0	0	0
$\hat{a}_{ty}(0)$	0	0	0
$\hat{a}_{tz}(0)$	0	0	0

It is obvious from Figs. 4, 5 and 6 that the range estimates are convergent for the accelerated target in scenarios 1 & 2 and for the non-accelerated target in the third scenario. Although almost similar results are observed for EKF and UKF methods in Figs. 4-6, range RMSE values for these two methods are computed and compared in Table 3, which shows that the UKF method performs slightly better than the EKF.

8 Conclusions

In this paper, PPNG is explained in a 3-dimensional state from a new point of view and then range estimation for passive homing missiles is explained. Simulation results indicate that the proposed tracking filters in conjunction with the proposed dual guidance law are able to provide the convergence of the range estimate in a few hundred meters for maneuvering and non-maneuvering targets. Simulation results showed that the UKF method performed slightly better than the EKF.

Table 3 Range RMSE comparisons for different scenarios.

	EKF	UKF
Scenario 1	5670 m	5464 m
Scenario 2	1590 m	1411 m
Scenario 3	1016 m	830 m

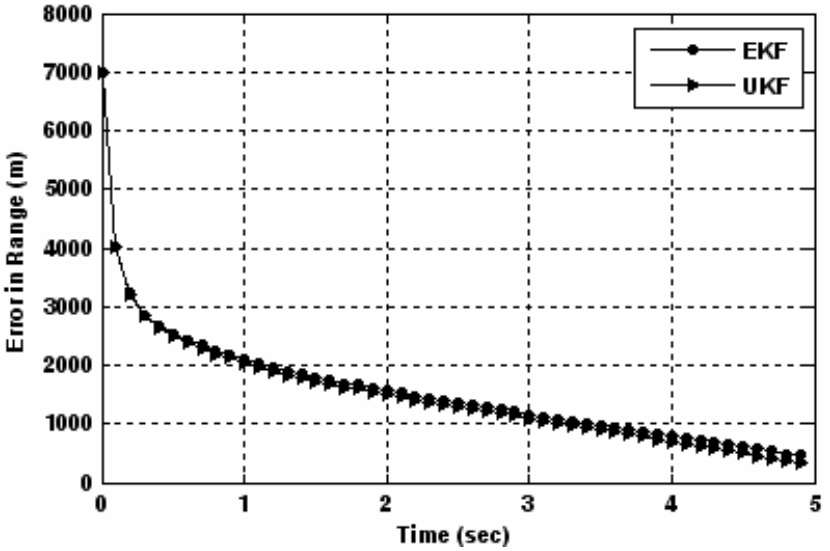

Fig. 4 Errors of the estimated range in scenario 1.

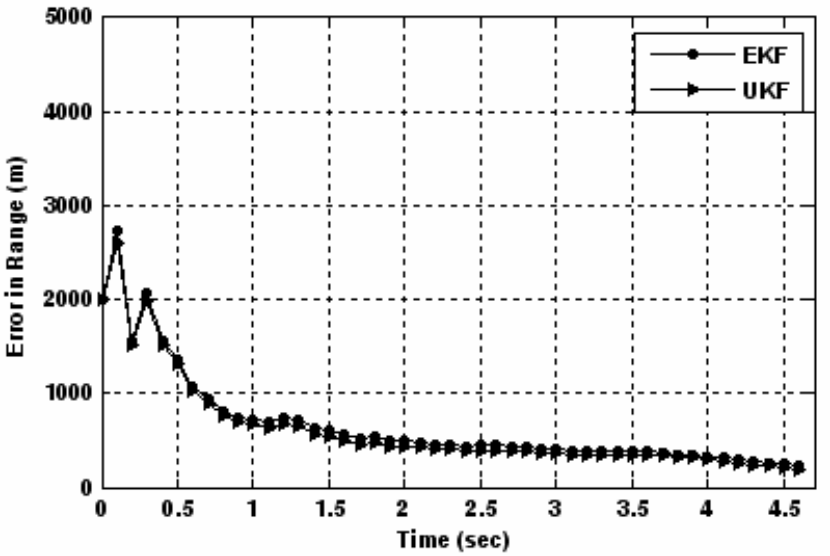

Fig. 5 Errors of the estimated range in scenario 2.

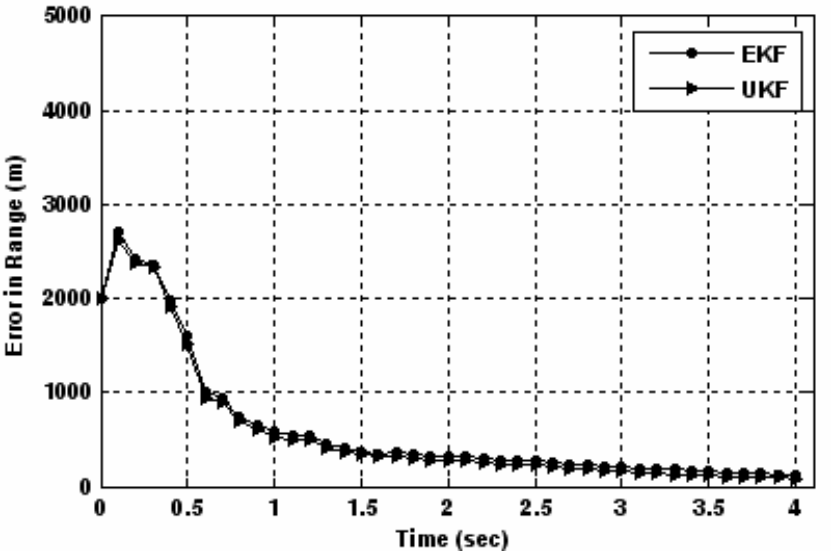

Fig. 6 Errors of the estimated range in scenario 3.

References

[1] Song T. L., "Target Adaptive Guidance for Passive Homing Missiles," *IEEE Transactions on Aerospace and Electronic Systems*, Vol. 33, No. 1, pp. 312-316, Jan. 1997.

[2] Taur D. R. and Chern J. S., "A Modified Proportional Navigation Guidance Law For IR Homing Missiles," *Proceedings of the AIAA Guidance, Navigation, and Control Conference*, AIAA-2000-4160, pp. 1-8, Aug. 2000.

[3] Karlsson R. and Gustafsson F., "Range Estimation using Angle-only Target Tracking with Particle Filters," *Proceedings of the American Control Conference*, pp. 3743-3748, June 2001.

[4] Lee S. Y., Kang S. J. and Kim D. J., "A Range Estimation Algorithm for Anti-Aircraft Artillery," *SICE-ICASE International Joint Conference*, pp. 796-801, Oct. 2006.

[5] Shukla U. S. and Mahapatra P.R., "The Proportional Navigation dilemma-pure or true?," *IEEE Transactions on Aerospace and Electronic Systems*, AES-26, pp. 382-392, Aug. 1990.

[6] Song S. H. and Ha I. J., "A Lyapunov-Like Approach to Performance Analysis of 3-Dimensional Pure PNG Laws," *IEEE Transactions on Aerospace and Electronic Systems*, Vol. 30, No. 1, pp. 238-247, Jan. 1994.

[7] Taur D. R. and Chern J. S., "Passive Ranging for Dog fight Air-to-Air IR Missiles," *Proceedings of the AIAA Guidance, Navigation, and Control Conference*, AIAA-99-4289, pp. 1737-1751, 1999.

[8] Kim P. S., Um T. Y. and Park H. B., "Passive Ranging in 3 Dimensional Homing Engagement," *SICE-ICASE International Joint Conference*, pp. 2924-2929, Oct. 2006.

[9] Song T. L. and Um, T. Y., "Practical Guidance for Homing Missile with Bearings-only Measurement," *IEEE Transactions on Aerospace and Electronic Systems*, Vol. 32, No. 1, pp. 434-443, Jan. 1996.

[10] Shneydor N. A., *Missile Guidance and Pursuit, Kinematics, Dynamics and Control*, Horwood Publishing Chichester, 1998, Appendix A.

[11] Tyan F., "Unified Approach to Missile Guidance Laws: A 3D extension,", *IEEE Transactions on Aerospace and Electronic Systems*, Vol. 41, No. 4, pp. 1178-1199, Oct. 2005.

[12] Ghose D., "On the generalization of true proportional navigation," *IEEE Transactions on Aerospace and Electronic Systems*, Vol. 30, pp. 545-555, Aug. 1994.

[13] Hudson R. D., *Infrared System Engineering*, John Wiley & Sons, New York, 1969, chapter 7.

[14] Simon D., *Optimal State Estimation: Kalman, H_∞, and Nonlinear Approaches*, John Wiley & Sons, New York, 2006, Chapter 6.

[15] Stallard D. V., "An Angle-Only Tracking Filter in Modified Spherical Coordinates," *Proceedings of the AIAA Guidance, Navigation, and Control Conference*, AIAA-87-2380, pp. 542-550, 1987.

[16] Zarchan P., *Tactical and Strategic Missile Guidance*, Third Edition, AIAA, 2002, Chapter 4.

[17] Robinsin P. N. and Yin M. R., "Modified Spherical Coordinates for Radar," *Proceedings of the AIAA Guidance, Navigation, and Control Conference*, AIAA-94-3546, pp. 55-64, 1994.

[18] Julier, S. J. and Uhlmann J. K., "A New Extension of the Kalman Filter to Nonlinear Systems," *Proceedings of AeroSense: The 11th Int. Symposium On Aerospace/Defense Sensing, Simulation and Controls*, Vol. Multi Sensor Fusion, Tracking and Resource Management II, 1997.

[19] Daum F., "Nonlinear Filters: Beyond the Kalman Filter," *IEEE A&E Systems Magazine*, Vol. 20., No. 8, pp. 57-69, Aug. 2005.

[20] Wan E. A. and Van der Merwe R., "The Unscented Kalman Filter for Nonlinear Estimation," *Proceedings of Symposium 2000 on Adaptive Systems for Signal Processing, Communication, and Control*, *IEEE*, pp. 153-158, 2000.

[21] Karlsson R. and Gustafsson F., "Recursive Bayesian estimation: Bearings-only Applications," *IEE Proceeding. on Radar, Sonar and Navigation*, Vol. 152, No. 5, pp. 305-313, Oct. 2005.

Ali Moharampour received his B.Sc. and M.Sc. degrees in Electrical Engineering from Tehran University, Tehran, Iran in 1996 and Iran University of Science and Technology, Tehran, Iran in 1999. He is presently pursuing the Ph.D. degree in Electrical Engineering, Iran University of Science and Technology. His research interests are estimation theory and nonlinear control theory.

Javad Poshtan received his B.Sc., M.Sc., and Ph.D. degrees in Electrical Engineering from Tehran University, Tehran, Iran, in 1987, Sharif University of Technology, Tehran, Iran, in 1991, and University of New Brunswick, Canada, in 1997, respectively. Since 1997, he has been with the Department of Electrical Engineering at Iran University of Science and Technology. He is involved in academic and research activities in areas such as control systems theory, system identification, and estimation theory.

Ali Khaki-Sedigh is a professor of control systems in the Electrical and Electronics Department of K. N. Toosi University of Technology in Tehran, Iran. He is the author and co-author of about fifty journal papers and has published seven books in the area of control systems in Persian. His main research interests are Adaptive and Robust Multivariable control systems, Chaos control and Hybrid systems, and also history of control.